

Efficient Photocurrent Generation by Self-Assembled Monolayers Composed of 3_{10} -Helical Peptides Carrying Linearly Spaced Naphthyl Groups at the Side Chains

Kazuyuki Yanagisawa, Tomoyuki Morita, and Shunsaku Kimura*

Department of Material Chemistry, Graduate School of Engineering, Kyoto University Kyoto-Daigaku-Katsura, Nishikyo-ku, Kyoto 615-8510, Japan

Received April 26, 2004; E-mail: shun@scl.kyoto-u.ac.jp

In natural photosynthetic systems, a regular arrangement of chromophores is a key for highly efficient light harvesting and charge separation.¹ Among secondary structures found in photosynthetic protein assemblies, the helical structure is most frequently observed and should play an important role in the regular arrangement of chromophores.² Further, the distance decay factor, β , for the electron transfer along a model helical peptide is reported to be $0.66 (\text{\AA}^{-1})$,³ which is better than alkane chains in the electron-mediated property.^{4,5} A helical peptide is thus used here as a scaffold of an artificial regular chromophoric array to attain an efficient long-range electron transfer. With respect to the distance between the chromophores, there should be a compromised distance of ca. 6\AA , in which electron transfer should be promoted by the "through space" mechanism³ and will not be hindered by energy-dissipating trap sites due to the formation of dimer or excimer.⁶ Taken together, the 3_{10} -helical structure, which makes one turn with just three residues, is chosen. When amino acids carrying chromophores at the side chains are introduced into a 3_{10} -helical peptide backbone at every third residue, the chromophores are regularly spaced in a linear manner along the helical axis. This linear and proximal arrangement of chromophores is expected to facilitate electron transfer between the adjacent chromophores. In the present study, self-assembled monolayers (SAMs) are prepared on gold from 3_{10} -helical peptides carrying naphthyl groups at the side chains, and photocurrent generation by the monolayers is discussed in terms of electron hopping among the naphthyl groups. Photocurrent generation by molecular assemblies has attracted much attention in relation to an artificial photosynthetic system.^{1,7,8}

A sequential nonapeptide carrying three naphthyl groups at the side chains of every third residue and a disulfide group at the N terminal, the reference peptide without a naphthyl group, and the peptides carrying one naphthyl group at N or C terminal (SSN3B, SSA3B, SSNA2B, SSA2NB, respectively; Figure 1) were synthesized. Since all the peptides are designed to contain six α -aminoisobutyric acid (Aib) residues, these peptides are expected to take a 3_{10} -helical conformation because of their high content of Aib residues.⁹ To examine the conformation of SSN3B in solution, its derivative BN3B, where the lipoic carbonyl group in SSN3B is replaced by the *tert*-butyloxycarbonyl group, was investigated by ¹H NMR spectroscopy in CDCl₃. The addition of (CD₃)₂SO to the solution induced the shift to the lower magnetic field of the urethane amide proton and one Aib amide proton. The result is consistent with this peptide taking a 3_{10} -helical conformation in chloroform. The same result was obtained for BA2NB as well. Geometry optimization using a MM2 method was applied to the acetyl-capped derivative of BN3B and also showed that 3_{10} -helical conformation is an energetically stable conformation as low as an α -helical conformation. In the energy-minimized 3_{10} -helical conformation, three naphthyl groups are spaced in a linear array along the helical axis with face-to-face orientation. The center-to-center distances

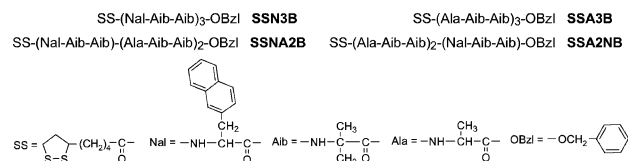


Figure 1. Chemical structures of SSN3B, SSA3B, SSNA2B, and SSA2NB.

between naphthyl groups are 6.1\AA for the first and fourth residue pair and 6.4\AA for the fourth and seventh pair, which are longer than the critical distance for excimer formation (ca. 3.5\AA). The space arrangement of the naphthyl groups is thus suitable for electron hopping without an energy-dissipating trap site. Further, circular dichroism spectroscopy of SSN3B showed an exciton coupling at around 223 nm in ethanol, which is characteristic of a regular arrangement of naphthyl groups in proximity in the 3_{10} -helical conformation.

To examine the electronic interaction between the naphthyl groups of SSN3B in the ground and excited states, absorption and fluorescence spectra were measured in ethanol. The absorption spectra of SSN3B showed the same pattern as that of SSA2NB, indicating that there is no strong electronic interaction in the ground state such as dimer formation. In the fluorescence spectrum of SSN3B, excimer emission was hardly observed, showing that there is no strong interaction in the excited state either. These observations agreed well with the prediction from geometry optimization. To summarize these results, the naphthyl groups of SSN3B are linearly spaced in proximity along the helical axis, but there is no trap site against electron hopping.

SAMs were prepared by immersion of a gold substrate into an ethanol solution of each peptide. The conformation and orientation of the peptides in the SAMs were investigated by infrared reflection absorption spectroscopy (IRRAS). Absorptions appeared at around 1670 and 1540 cm^{-1} in the IRRAS spectra for the SAMs, which were assigned to amide I and amide II absorptions of helical conformation, respectively.¹⁰ Calculations based on the amide I/II absorption ratio gave the tilt angles of the helical axis from the surface normal of 31° , 47° , 57° , and 36° for the SSN3B, SSA3B, SSNA2B, and SSA2NB SAMs, respectively. To examine the molecular packing of the SAMs, cyclic voltammetry was performed in an aqueous $\text{K}_4[\text{Fe}(\text{CN})_6]$ solution. Especially, the SSN3B SAM showed negligible peaks of the Fe(III)/Fe(II) redox couple compared with the case of a bare gold substrate, indicating that the SSN3B SAM is tightly packed without any defects. Similar results were obtained for the SSA3B and SSNA2B SAMs. On the other hand, the SSA2NB showed relatively large peaks, showing that the SSA2NB SAM is loosely packed. On the basis of these data, it was suggested that the three naphthyl groups of SSN3B promote vertical orientation and dense packing of helical peptides in the SAM.

Photocurrent generation by these peptide SAMs was investigated by photoexcitation of the naphthyl group in an aqueous solution

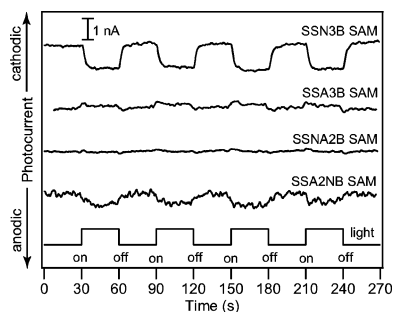


Figure 2. Photocurrent generation upon light irradiation at 280 nm (1.2×10^{14} photons s^{-1}) at applied potential of 0 V vs Ag/AgCl reference electrode. The irradiated area of electrode was ca. 0.2 cm^2 . The measurements were carried out in an aqueous 50 mM TEOA solution.

containing triethanolamine (TEOA) as an electron donor. Significant anodic photocurrent generation was successfully observed on the SSN3B SAM in response to photoirradiation (Figure 2). The action spectrum of the SSN3B SAM agreed well with the absorption spectrum of SSN3B in ethanol, showing that the naphthyl groups act as sensitizer for the photocurrent generation. The quantum efficiency of the photocurrent generation was found to be 2.1%, which is a moderate value for the long-range electron transfer.^{7,8} On the other hand, no anodic photocurrent was generated by the SSA3B or SSNA2B SAM, and only indistinct photocurrent was observed in the SSA2NB SAM, which was at most one-third of that by the SSN3B SAM. The low signal/noise ratio in the photocurrent of the SSA2NB SAM should arise from the loose packing of the monolayer because the bare gold area exposed to the aqueous solution is sensitive to the environmental electric noises since the bare gold substrate shows large noises.

Noticeably, the SSNA2B SAM showed almost no photocurrent signal, but a weak photocurrent generation was observed in the SSA2NB SAM. The reason for this difference between the reference SAMs (with one naphthyl group) may be explained as follows. There are two steps for the anodic photocurrent generation; one is the photoinduced electron transfer from the photoexcited naphthyl group to gold, and the other is the subsequent electron donation from TEOA to the oxidized naphthyl group. It is considered that the photoexcited naphthyl group in the both SAMs can donate an electron easily to gold because of the large energy difference between the redox potential of the photoexcited naphthyl group and the Fermi level of gold. However, the subsequent electron donation from TEOA to the radical cation of the naphthyl group needs diffusion of TEOA in aqueous phase to the naphthyl group in the SAMs. The diffusion is strongly suppressed in the case of the SSNA2B SAM to generate no photocurrent. The other possible reference monolayer, where one naphthyl group is located at the middle site, was not examined in this study; however, the photocurrent can be roughly estimated to be in between those by SSNA2B and SSA2NB SAMs due to the intermediate distance between TEOA in aqueous phase and the naphthyl group in the SAM. The photocurrent by the SSN3B SAM is then at least two times larger than the sum of the photocurrents by these three reference SAMs. It is therefore concluded that electron hopping among the linearly-spaced naphthyl groups effectively promotes the photocurrent generation in the SSN3B SAM. A representative case is shown in Figure 3, where the naphthyl group at the site nearest to gold is photoexcited. In this case, the radical cation, which is generated by photoinduced electron transfer from the naphthyl group to gold, subsequently hops away from gold via the naphthyl groups and finally is quenched by electron donation from TEOA in an aqueous phase. Further, the electron hopping process should be promoted by effective mediation of electron transfer by a helical

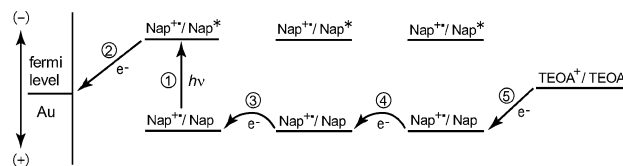


Figure 3. Energy diagram for anodic photocurrent generation by the SSN3B SAM in the case that the naphthyl group at the site nearest to gold is excited by photoirradiation.

peptide backbone^{3,11} and might be accelerated by the dipole moment of the helix, since it has been shown that the dipole moment with the same direction as that of electron transfer accelerates the electron transfer in α -helical peptides.^{5,12} In addition, energy migration among the naphthyl groups may promote the photocurrent generation, because the distance between the neighboring naphthyl groups (ca. 6 Å) is shorter than the critical distance between naphthyl groups for energy migration of the Förster type (8.3 Å). These effects on the photocurrent generation are to be examined in a future report.

In summary, we prepared SAMs from a novel 3_{10} -helical peptide carrying three naphthyl groups of a regular and linear arrangement with the reference peptides carrying no or one naphthyl group at the terminal residue. The SAM prepared from the peptide carrying three naphthyl groups was shown to have a well-packed structure and vertical molecular orientation. The photocurrent generation experiment revealed that the linearly spaced naphthyl groups along the helical axis effectively increase the photocurrent by photosensitization and electron hopping between the naphthyl groups. To our knowledge, this is the first example of a three-dimensional arrangement (linear array) of functional groups in a self-assembled monolayer system accomplished by utilizing the regular structure of a 3_{10} -helical peptide, that cannot be realized by conventional sulfur-terminated compounds. We are now examining the distant electron-transfer reactions in 3_{10} -helical peptides carrying chromophores at the side chains.

Acknowledgment. This work is partly supported by a Grant-in-Aid for Young Scientists B (14750694), Priority Areas Research B (Construction of Dynamic Redox Systems Based on Nano-Space Control), and 21st Century COE program, COE for a United Approach to New Materials Science, from the Ministry of Education, Culture, Sports, Science, and Technology.

Supporting Information Available: Details in synthesis, spectroscopic and electrochemical measurements. This material is available free of charge via the Internet at <http://pubs.acs.org>.

References

- Wasielowski, M. R. *Chem. Rev.* **1992**, *92*, 435–461.
- Beratan, D. N.; Onuchic, J. N.; Winkler, J. R.; Gray, H. B. *Science* **1992**, *258*, 1740–1741.
- Sisido, M.; Hoshino, S.; Kusano, H.; Kuragaki, M.; Makino, M.; Sasaki, H.; Smith, T. A.; Ghiggino, K. P. *J. Phys. Chem. B* **2001**, *105*, 10407–10415.
- Fox, M. A.; Galoppini, E. *J. Am. Chem. Soc.* **1997**, *119*, 5278–5279.
- Morita, T.; Kimura, S.; Kobayashi, S.; Imanishi, Y. *J. Am. Chem. Soc.* **2000**, *122*, 2850–2859.
- Morita, T.; Kimura, S.; Imanishi, Y. *J. Am. Chem. Soc.* **1999**, *121*, 581–586.
- Uosaki, K.; Kondo, T.; Zhang, X.-Q.; Yanagida, M. *J. Am. Chem. Soc.* **1997**, *119*, 8367.
- Imahori, H.; Yamada, H.; Nishimura, Y.; Yamazaki, I.; Sakata, Y. *J. Phys. Chem. B* **2000**, *104*, 2099–2108.
- Karle, I. L.; Sukumar, M.; Balaram, P. *Proc. Natl. Acad. Sci. U.S.A.* **1986**, *83*, 9284–9288.
- Kennedy, D. F.; Chrisma, M.; Chapman, T. D. *Biochemistry* **1991**, *30*, 6541–6548.
- Isied, S. S.; Ogawa, M. Y.; Wishart, J. F. *Chem. Rev.* **1992**, *92*, 381–394.
- Galoppini, E.; Fox, M. A. *J. Am. Chem. Soc.* **1996**, *118*, 2299–2300.

JA0476011